International Journal of Heat and Mass Transfer 160 (2020) 120175

Contents lists available at ScienceDirect

International Journal of Heat and Mass Transfer

journal homepage: www.elsevier.com/locate/hmt

Evaluation of heat transfer models at various fluidization velocities for biomass pyrolysis conducted in a bubbling fluidized bed

Lukas von Berg[a,*], Antonio Soria-Verdugo[b], Christoph Hochenauer[a,c], Robert Scharler[a,c], Andrés Anca-Couce[a]

[a] Institute of Thermal Engineering, Graz University of Technology, Inffeldgasse 25/B, 8010 Graz, Austria
[b] Carlos III University of Madrid, Energy Systems Engineering Group, Thermal and Fluids Engineering Department, Avda. de la Universidad 30, 28911 Leganés, Madrid, Spain
[c] BEST – Bioenergy and Sustainable Technologies GmbH, Inffeldgasse 21b, 8010 Graz, Austria

ARTICLE INFO

Article history:
Received 27 May 2020
Revised 2 July 2020
Accepted 7 July 2020

Keywords:
Fluidized bed
Heat transfer
Modeling
Biomass
Pyrolysis

ABSTRACT

Four different models for heat transfer to the particles immersed in a fluidized bed were evaluated and implemented into an existing single particle model. Pyrolysis experiments have been conducted using a fluidized bed installed on a balance at different temperatures and fluidization velocities using softwood pellets. Using a heat transfer model applicable for fluidized beds, the single particle model was able to predict the experimental results of mass loss obtained in this study as well as experimental data from literature with a reasonable accuracy. A good agreement between experimental and modeling results was found for different reactor temperatures and configurations as well as different biomass types, particle sizes – in the typical range of pellets - and fluidization velocities when they were higher than $U/U_{mf} = 1.5$. However, significant deviations were found for fluidization velocities close to minimum fluidization. Heat transfer models which consider the influence of fluidization velocity show a better agreement in this case although differences are still present.

1. Introduction

In order to tackle climate change, we need to limit the temperature rise in this century to 1.5 K above preindustrial levels [1]. Biomass as a source of renewable energy plays an important role if we want to meet this main goal of the Paris Agreement. Pyrolysis and gasification represent alternative routes of biomass conversion with many possible applications when compared to combustion. The biooil produced during pyrolysis can be used as a liquid biofuel in diesel engines after an upgrade or to produce biobased chemicals [2]. Besides, the obtained biochar in pyrolysis has as well several applications [3]. The producer gas obtained during gasification is applicable in a gas engine or a fuel cell to produce power with high efficiencies, but can also be used for production of chemicals or biofuels [4]. Fluidized beds represent a promising technology to conduct fast pyrolysis or gasification of biomass. Advantages are the easy scale-up to medium and large scale plants [4], the homogeneous temperature distribution inside the bed and the very high heat transfer coefficient to the solid fuel due to intensive particle-particle-interaction. However, the combination of complex bed hydrodynamics, intra-particle gradients and complicated gas phase kinetics make it difficult to fully understand and optimize the process. Modeling tools, together with experimental work, can help to get a profound overview of the processes in a fluidized bed and thereby support the development of this technology.

Many different modeling approaches are used in literature and a comprehensive overview about gasification modeling in fluidized beds is given by Gomez-Barea and Leckner [4]. Single particle models aim to describe the processes inside the fuel particles and usually rely on a large amount of input parameters and sub-models which have a significant impact on the modeling results. The review about modeling of biomass pyrolysis by Di Blasi [5] gives an insight of available sub-models. For the case of a fluidized bed reactor, special attention needs to be payed to the heat transfer between bed material and fuel particles, which differs to a great extent from the heat transfer to a single sphere or a fixed bed.

Several studies available in literature investigate the heat transfer in a fluidized bed [5]. Kersten et al. [6] applied a single particle model for pyrolysis of biomass cylinders considering boundary conditions typical for a fluidized bed. The influence of heat transfer

* Corresponding author.
E-mail address: lukas.vonberg@tugraz.at (L. von Berg).

https://doi.org/10.1016/j.ijheatmasstransfer.2020.120175

Nomenclature

Ar_i	Archimedes number of inert particle [-]
Bi	Biot number [-]
$c_{p,\,g}$	heat capacity of gas [J/(kg*K)]
d	diameter of biomass pellet [m]
d_a	diameter of active particle (biomass) [m]
d_i	diameter of inert particle (bed material) [m]
g	acceleration due to gravity [m/s^2]
h	heat transfer coefficient [W/(m^2*K)]
h_{bub}	heat transfer coefficient to the particle while being in the bubble phase [W/(m^2*K)]
h_{gc}	gas convective heat transfer coefficient [W/(m^2*K)]
$h_{\max}$	heat transfer coefficient calculated via Nusselt correlation of Prins [W/(m^2*K)]
h_{pc}	particle convective heat transfer coefficient [W/(m^2*K)]
$h_{pc,a}$	particle convective heat transfer coefficient during ascent [W/(m^2*K)]
$h_{pc,d}$	particle convective heat transfer coefficient during descent [W/(m^2*K)]
L	length of biomass pellet [m]
L_c	characteristic length [m]
m	mean particle mass [g]
Nu_1	Nusselt correlation by Palchonok [-]
Nu_i	Nusselt correlation (averaged Baskakov-Palchonok) [-]
$Nu_{i,\,\max}$	Nusselt correlation by Prins [-]
$Nu_{i,\,\infty}$	Nusselt correlation by Baskakov [-]
p	probability of the active particle residing in the emulsion phase during one circulation [-]
p'	probability of the active particle residing in the emulsion phase while it rises during one circulation [-]
Pr	Prandtl number [-]
R_c	surface contact resistance [m^2*K/W]
R_p	thermal resistance of the thermal penetration layer [m^2*K/W]
R_s	resistance to heat transfer [m^2*K/W]
R_{th}	thermal resistivity in the solid material [m^2*K/W]
T	reactor temperature [K]
U	fluidization velocity [cm/s]
U_{mf}	minimum fluidization velocity [cm/s]
X_{char}	char yield [-]

Greek letters

$\lambda_{biomass}$	thermal conductivity of biomass [W/(m*K)]
λ_{char}	thermal conductivity of char [W/(m*K)]
λ_g	thermal conductivity of gas [W/(m*K)]
ρ_g	density of gas [kg/m^3]
ρ_i	density of inert bed material [kg/m^3]
μ_g	dynamic viscosity of gas [kg/(m*s)]

Abbreviation

HTM	heat transfer model

coefficient and particle diameter on the conversion time was investigated. The heat transfer coefficient was varied in a range between 50 and 1200 W/(m^2*K) and it showed a clearly noticeable influence for small particles with diameters ranging from 1 to 3 mm. The reaction regime for these small particles approaches the kinetically controlled regime due to the high heat transfer coefficient in fluidized beds. For particles bigger than 5 mm, the model predicted a comparably smaller influence of heat transfer coefficient on the conversion time. Heat conduction seems to be the main limiting factor in the heating process. However, it is stated that the effect of the heat transfer on the conversion time for these particles can still be as high as 20%. Therefore, a more detailed investigation including the use of heat transfer models is needed.

Di Blasi [7] developed a single particle model of cellulose pyrolysis coupled with a mechanistic external heat transfer model from Agarwal [8]. Additionally, two simplified approaches of modeling heat transfer were investigated. Heat transfer was calculated using the Ranz-Marshall model as well as with the assumption of an infinitely fast heat transfer rate. The Agarwal model lead to heat transfer coefficients between 480 and 1880 W/(m^2*K) when varying the particle diameter from 10 to 0.2 mm whereas the Ranz-Marshall model gave values between 22 and 650 W/(m^2*K). As the Ranz-Marshall correlation only considers the gas convective contribution, the heat transfer coefficient is lower. For thick particles, the Agarwal model leads to heat transfer coefficients up to 22 times bigger than with the Ranz-Marshall model. The study concludes that correct estimations of process characteristics like heating rate, conversion time and product distribution cannot be based on any of the two simplifications (Ranz-Marshall or infinitely fast heat transfer).

A general approach of external heat transfer modeling to the particle different than the one of Agarwal [8] is presented by Gómez-Barea and Leckner [4]. It is based on Nusselt correlations to calculate the heat transfer coefficient from an inert bed material to an active biomass particle in fluidized beds. Two limiting cases are presented. One correlation is valid for large active particles in a bed of smaller particles. The other correlation describes heat transfer to active particles which are about the same size as the bed material. Interpolation between these two cases leads to a Nusselt number which allows to calculate the heat transfer coefficient.

In another study, Gómez-Barea et al. [9] investigated the devolatilization of wood and wastes in fluidized beds and a simplified model is presented. The model is validated with experiments conducted using dried sewage sludge of 1.2–4.5 mm diameter and wood particles of 6 mm diameter. The temperature profile during heating up of a particle was calculated while thermal effects of pyrolysis and drying were neglected. Also fuel properties and particle size were kept constant based on the assumption that simultaneous effects compensate each other. The heat transfer coefficient was considered using two different correlations which are the Nusselt correlation by Ranz-Marshall as well as a correlation specifically derived for fuel conversion in a fluidized bed. The model derived in [4] is employed but without interpolation between the two limiting cases described in the previous paragraph. Instead, the heat transfer coefficient used for simulations was averaged between the correlation of Ranz-Marshall and one of the fluidized bed correlations. Representative values for the heat transfer coefficient are 160 W/(m^{2}K) for wood pellets and between 185 and 250 W/(m^{2}K) for dried sewage sludge particles. They observed that the heat-up of the dried sewage sludge particles was mainly influenced by external heat transfer. For wood pellets both internal and external heat transfer were found to be important. Moreover, experiments were conducted using 4.5 mm dried sewage sludge particles at 750 and 800 °C and two different fluidization velocities of 0.55 and 0.8 m/s. For lower fluidization velocities, the conversion is slower indicating a significant influence by external heat transfer. However, modeling of these cases was not conducted.

Some of the recently developed heat transfer models for fluidized beds are based on artificial neural networks [10] or fuzzy logic [11]. However, these models presented in literature focus on particle-wall heat transfer and are not directly applicable in the current paper. For future research, such models might be interesting as they sometimes overcome the shortcomings of the more

common models like the need of additional input data and long calculation times [11].

Besides the previous works, further experimental studies investigating biomass pyrolysis in fluidized beds are present in literature. Di Blasi and Branca [12] measured the temperature at the center of solid hardwood particles with a fixed thermocouple which is located in a fluidized bed. The influence of particle size and temperature were investigated. Reschmeier et al. [13] used a fluidized bed placed on a balance to measure mass loss of softwood particles during pyrolysis at different temperatures. However, the influence of the fluidization velocity was not investigated by Reschmeier et al. Experiments by Morato-Godino et al. [14] were conducted in order to investigate the influence of particle size, reactor temperature and fluidization velocity for cardoon pellets. However, experimental studies investigating the influence of fluidization velocity on the pyrolysis of wood pellets in a fluidized bed are hard to find.

As there are several approaches to model external heat transfer in literature, the goal of this study is to evaluate different heat transfer models to describe pyrolysis of a single particle in a fluidized bed at different conditions. Therefore, the single particle model for biomass pyrolysis developed by Anca-Couce et al. [15] was used. The model employs a detailed reaction mechanism based on the primary pyrolysis scheme of Ranzi et al. [16] which was updated by Corbetta et al. [17], extended by secondary charring reactions and further improved by adaptions based on experimental results. The pyrolysis model was already intensively tested for slow pyrolysis [15] and results in an accurate representation of mass loss curves. For the work conducted in this study, it is therefore assumed that pyrolysis is accurately described. Deviations to experimental data in this work are therefore not attributed to the pyrolysis model but to the heat transfer model. The main adaption at the particle scale necessary to make the model applicable for fluidized bed reactors is the heat transfer to the particle. Due to the intense particle contact in a fluidized bed, it can be orders of magnitudes higher compared to a particle in a fixed bed reactor. Therefore, four different heat transfer models by Prins [18], Baskakov-Palchonok [4], Agarwal [8] and Chao [19] were implemented and validated with experimental data (Section 2). The adapted single particle model was compared to experimental data published by Di Blasi and Branca [12], Reschmeier et al. [13] and Marato-Godino et al. [14]. Experimental data of wood pellet pyrolysis in a fluidized bed while varying the fluidization velocities can hardly be found in literature. Therefore, mass loss measurements using a fluidized bed TGA and softwood pellets were conducted in this study (Section 3). The influence of different bed temperatures and fluidization velocities on the mass loss was investigated and the experimental results were used to evaluate the different heat transfer models (Section 4).

2. Evaluation of heat transfer models

In the following chapter, four different heat transfer models are evaluated. These models were later implemented in the single particle model and compared to experimental data of biomass particles pyrolyzing in a fluidized bed. The models are based on different approaches and some of them consider the effect of the fluidization velocity whereas no effect of gas velocity is considered in others. The models either calculate the heat transfer coefficient h directly or give a correlation for the Nusselt number. The heat transfer coefficient can then be calculated via the definition of the Nusselt number were d is the particle diameter and λ_g the thermal conductivity of the gas phase.

$$h = Nu * \frac{\lambda_g}{d} \tag{1}$$

A heat transfer model based on measurements of heat transfer to fixed or freely moving graphite or silver spheres immersed in a gas fluidized bed of smaller glass particles was presented by Prins [18]. The measurements were conducted by connecting the sphere to either a stiff thermocouple (which results in a fixed position of the sphere in the bed) or a long thin thermocouple (which leads to an almost free movement of the sphere in the bed). For both conditions, a correlation for the maximum heat transfer coefficient at optimal fluidization conditions was developed and it was found that the difference between freely moving and fixed sphere was rather small (less than 10%). However, recent research in the field of char combustion using a visual technique based on pyrometry coupled with a digital camera showed, that the influence of the thermocouple on the movement of particles is not negligible [20]. In this study, the correlation derived for freely moving spheres was used. The correlation for the Nusselt number $Nu_{i,\,max}$ at optimal fluidization conditions is calculated as shown below via the Archimedes number Ar_i as well as the ratio of the sphere diameter d_a to bed material diameter d_i. Moreover, g is the acceleration due to gravity, ρ_i is the density of the inert bed material and ρ_g, μ_g and λ_g are the density, the dynamic viscosity and the thermal conductivity of the gas. The influence of the fluidization velocity is not considered. Furthermore, no influence of radiation on the heat transfer was found for temperatures up to 1173 K.

$$Ar_i = g * d_i^3 * \rho_i * (\rho_i - \rho_g) * \mu_g^2 \tag{2}$$

$$Nu_{i,\max} = 3.539 * Ar_i^n \left(\frac{d_a}{d_i}\right)^{-0.257} \quad where\ n = 0.105\left(\frac{d_a}{d_i}\right)^{0.082} \tag{3}$$

A mechanistic model for heat transfer to an active, freely moving particle in a fluidized bed was developed by Agarwal [8]. The model is based on findings for the heat transfer to fixed tubes in a fluidized bed. It was originally developed to model fluidized bed combustion but can also be used to simulate fast pyrolysis in a fluidized bed [5]. During its circulation in the bed, the active particle can either be located in the emulsion phase or in a bubble. The model assumes that there are four different conditions which are considered to calculate the overall heat transfer. The effect of radiation is not considered in the model. Furthermore, modeling work of Di Blasi [7] showed that radiation plays a negligible role when combined with the heat transfer model of Agarwal. The particle convective heat transfer coefficient is divided into $h_{pc,a}$ for the ascent and $h_{pc,d}$ for the descent of the active particle in the bed. The gas convective heat transfer coefficient h_{gc} considers heat transfer from the gas to the particle while it is in the emulsion phase and h_{bub} respects the heat transfer to the particle while being in the bubble phase. These four contributions are weighted with probabilities and combined to calculate the average heat transfer coefficient h to a single particle.

$$h = p' * h_{pc,a} + \left(p - p'\right) * h_{pc,d} + p * h_{gc} + (1 - p) * h_{bub} \tag{4}$$

Here, p is the probability of the particle being in the emulsion phase during one circulation and p' is the probability of the particle being in the emulsion phase while it rises during one circulation. More details about the model and all required equations can be found in [8]. Comparison of the model estimations with the experimental data of Prins [18] shows good agreement for different particle sizes and fluidization velocities.

A combination of the models of Palchonok et al. [21] and Baskakov et al. [22] is presented by Gómez-Barea and Leckner [4], where the heat transfer coefficient is interpolated between two limiting cases as shown in Eq. (5). The heat transfer for a large fixed rounded object in a fluidized bed can be calculated via the Baskakov correlation shown in Eq. (6) and presents the lower limit of the heat transfer coefficient. The Archimedes number Ar_i is cal-

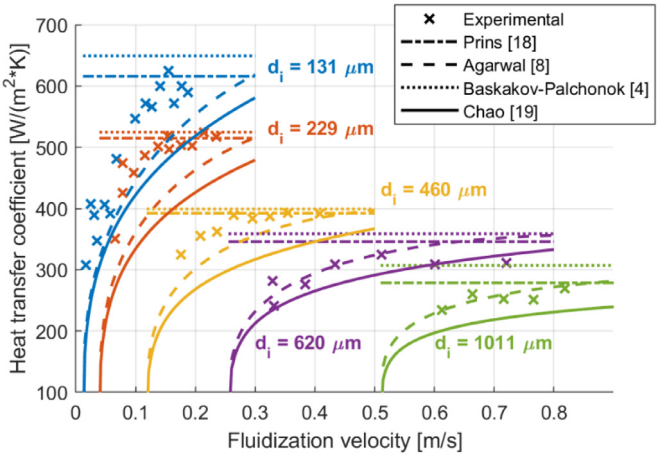

Fig. 1. Comparison of heat transfer models in dependence of fluidization velocity for different bed material diameters (15 mm graphite sphere in a fluidized bed of glass beads at a temperature of 573 K).

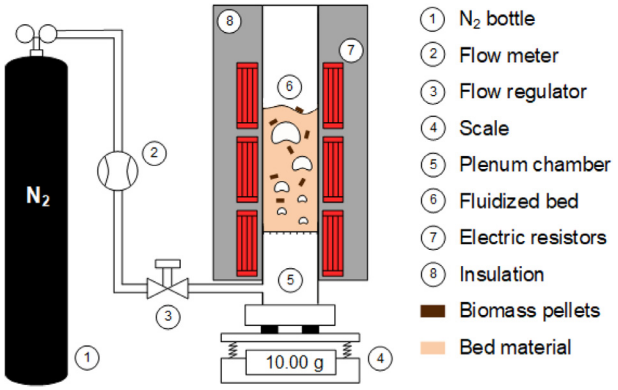

Fig. 2. Experimental set-up of the electrically heated fluidized bed on a balance.

culated as shown above and the Prandtl number is defined as $Pr = c_{p,g} * \frac{\mu_g}{\lambda_g}$. The model by Palchonok et al. [21] is valid for very small active particles in an inert bed and corresponds to the upper limit of heat transfer. The Nusselt number for this case is presented in Eq. (7).

$$Nu_i = h * \frac{d_i}{\lambda_g} = Nu_{i,\infty} + (Nu_1 - Nu_{i,\infty}) * \left(\frac{d_i}{d_a}\right)^{0.66} \quad (5)$$

$$Nu_{i,\infty} = 0.85 * Ar_i^{0.19} + 0.006 * Ar_i^{0.5} * Pr^{0.33} \quad (6)$$

$$Nu_1 = 6 + 0.117 * Ar_i^{0.39} * Pr^{0.33} \quad (7)$$

A recently developed model by Chao et al. [19] is based on the surface resistance model. The total heat transfer coefficient is calculated as the sum of particle convective heat transfer h_{pc} and gas convective heat transfer h_{gc}. The model does not include effects of radiation on the heat transfer coefficient.

$$h = h_{pc} + h_{gc} = \frac{1}{R_c + R_p} + h_{gc} \quad (8)$$

Where R_c is the surface contact resistance, which can be considered as the conductive thermal resistance through a gas layer. The mean conduction path is derived from experimental data by Chao et al. [19]. R_p is the thermal resistance of the thermal penetration layer which is mainly controlled by the mean emulsion residence time which is a function of bed material diameter, fuel diameter and fluidization velocity [19]. Measurements of heat transfer coefficients were conducted to determine input parameters necessary to calculate R_c and R_p and validation with the experimental data of Prins [18] showed good agreement of the heat transfer coefficients for different particle sizes and gas velocities. Furthermore, the model was recently validated with experimental measurements of dry ice sublimation conducted in a fluidized bed reactor located on a balance [23].

A comparison of all of the previously introduced models to the experimental data of Prins [18] is shown in Fig. 1. The experimental data was obtained by measuring the temperature of a 15 mm graphite sphere via a flexible thermocouple in a fluidized bed of glass beads at a temperature of 573 K. Measurements were conducted for bed material diameters ranging from $d_i = 131,\ 229,\ 460,\ 620\ to\ 1010\ \mu m$ while the fluidization velocity was varied for each diameter. For 131 and 229 μm particles, the effect of fluidization velocity is very strong and heat transfer coefficients above 500 W(m^2*K) are reached. For bigger bed material particles, a similar effect was observed, however with a much smaller increase of the heat transfer coefficient. The model of Prins (dash-dotted line), as well as the model of Baskakov-Palchonok (dotted line) consider no influence of varying fluidization velocity which leads to a high error at low fluidization velocities. The model of Agarwal (dashed line) shows good agreement with the experimental data, but especially for small bed material particle diameters, the deviation to the measured values is more distinct. For high fluidization velocities, the Agarwal model reaches values close to the model of Prins as well as to the Baskakov-Palchonok model. The model of Chao (solid line) shows a similar trend in terms of velocity dependency as the Agarwal model. However, the heat transfer coefficients are a bit lower. In conclusion, the Agarwal model seems to be able to represent the heat transfer coefficient with high accuracy for most of the cases. Therefore, it will be used as the reference model to estimate heat transfer coefficients to solid particles freely moving inside a fluidized bed in the following modeling work.

3. Materials and methods

3.1. Experimental

In order to validate the model, a series of experimental pyrolysis tests of softwood pellets in a nitrogen blown fluidized bed were conducted. The tests were performed using a fluidized bed located on a balance. This allows to measure the mass loss of the pellets due to the devolatilization during the pyrolysis process. These mass loss curves were then compared to the modeled mass loss. A scheme of the experimental setup is shown in Fig. 2. The electrically heated fluidized bed with an inner diameter of 47 mm is located on a balance and N_2 is fed from the bottom as fluidization agent. The N_2 is preheated in the plenum chamber to the bed temperature via an electric resistor. All connections to the reactor are designed carefully to minimize the influence on the measurement signal.

In the following section, the characterization of the used biomass and bed material, the experimental setup as well as the experimental procedure is explained.

3.1.1. Basic characterization of the pellets

Commercial softwood pellets with a diameter of 6 mm and a density of 1213 kg/m^3 were used as fuel. The results of proximate and ultimate analysis are shown in Table 1. The proximate analysis was carried out in a TGA Q500 from TA Instruments using pulverized wood obtained from the pellets. The particle size employed was below 100 μm and the sample initial mass was 10 mg

Table 1
Basic characterization of the softwood pellets (wb: wet basis, *: difference to 100%).

Proximate analysis			Ultimate analysis			
Moisture	Volatile matter (at 1173 K)	Fixed-carbon (at 1173 K)	C	H	N	O*
[m%wb]	[m%wb]	[m%wb]	[m%wb]	[m%wb]	[m%wb]	[m%wb]
5.26	79.98	14.76	46.72	6.33	0.27	46.68

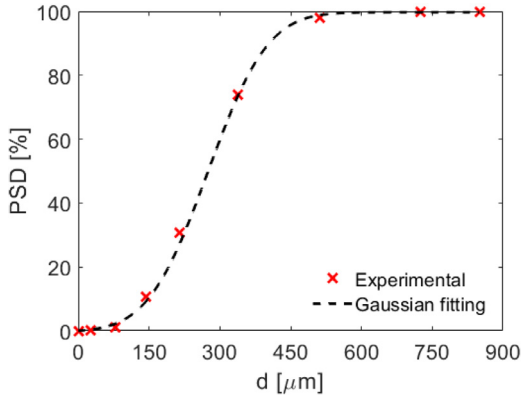

Fig. 3. Particle size distribution of the bed material employed.

to avoid heat and mass transfer in the sample. For the characterization of the char content, the temperature was raised up to 1173 K with a constant heating rate of 25 K/min. The elemental analysis of the wood pellets was conducted in a LECO TruSpec CHN analyzer.

3.1.2. Bed material

The bed material employed for the experiments was silica sand with a particle size distribution shown in Fig. 3. The corresponding Gaussian distribution is characterized by an average value of 275 μm and a standard deviation of 100 μm.

The particle density of the silica sand is 2600 kg/m^3. The bulk density of the bed material employed was measured to be 1576.3 kg/m^3. A total mass of 257 g of fresh silica sand was used for each test, corresponding to a static bed height of 9.4 cm, i.e., twice the reactor inner diameter. The minimum fluidization velocity was measured for each temperature as the velocity for which bubbles start to appear in the bed surface. The results for U_{mf} are 3.81, 3.75 and 3.72 cm/s at 673 K, 773 K and 873 K, respectively.

3.1.3. Operating conditions and experimental procedure

Experiments at seven different conditions were conducted in order to investigate the influence of operating temperature, fluidization velocity and particle dimensions. For each operating condition, three tests were run to evaluate the repeatability of the experimental procedure. Two of the replicates were run pyrolyzing 5 pellets. The third replicate was carried out using 10 pellets of similar geometry to double the initial mass and therefore, reducing the effect of vibration due to bubbles. For all cases, the repeatability of the tests was acceptable. Furthermore, it was observed that doubling the number of pellets has no influence on the overall pyrolysis behavior, but led to a more stable mass signal with lower effect of fluctuations. Therefore, in the present study, only the data of the test using 10 pellets as the initial mass were used.

The conditions for all experiments are summarized in Table 2. For each test, the operating temperature of the fluidized bed and the fluidization conditions are presented. The particle diameter d is 6 mm and the mean particle length L was calculated via the particle mass and density. Tests 1 to 6 were conducted with a particle length of about $L = 22$ mm. Test 7 was performed with a pellet length of $L = 8.3$ mm to investigate the influence of the particle dimensions. In order to improve the quality of the measured signal, this test was carried out using 30 pellets, which lead to an initial mass of 8.5 g. The repeatability of the tests with the short pellets was also acceptable, similar to that obtained with the long pellets. For each experiment except for test 2 and 7, the char particles were extracted from the bed after it was cooled down below 423 K while keeping the flow-rate of nitrogen same as during the test. The char particle dimensions were analyzed using digital image processing. Furthermore, the total mass of the char particles was measured and the mass fraction of char X_{char} was calculated. The char yield is inversely proportional to both reactor temperature and gas velocity.

Main error sources of the measurement technique can be attributed to the bubbles rising in the bed. As high fluidization velocities lead to vigorous bubbling, the fluctuations of the mass signal detected at the balance got stronger and accuracy of the measurements was lower. However, repetition of the experiments showed good repeatability and therefore, mean values complemented by their standard deviation were used. As the mass of the inert bed material was very high compared to the mass of fuel and the thermal inertia of the reactor vessel and electric resistors is high, the temperature of the bed was assumed to stay constant during each experiment. Therefore, the influence of temperature fluctuations of the bed on the measured mass signal during each test was assumed to be negligible.

3.2. Modeling

The single particle model used in this study is a one-dimensional volumetric model with a discretization of 20 grid points [15]. The reaction kinetics are based on the pyrolysis scheme developed by Ranzi et al. [16]. The model assumes that cellulose, hemicellulose and three types of lignin present in biomass decompose independently. The model, originally developed by Anca-Couce et al., was already extensively tested for fixed-bed pyrolysis in lab-scale reactors [24]. The model was also used to describe the torrefaction of softwood and hardwood particles and it was validated with experiments in a lab-scale reactor using spruce and beech particles [25]. Besides, for measurements using a single particle reactor, the latest version of the model can predict the yields and online release of CO, CO_2, H_2O, CH_4, other light hydrocarbons and total organic condensable species, as well as char yield with reasonable accuracy [15]. Representative initial compositions of softwood and hardwood as proposed in [25], together with relevant model properties, are shown in Table 3. The initial porosity was adapted for each fuel investigated in this study in order to ensure a correct value for the particle density.

The original model used the correlation of Churchill-Bernstein [26] to calculate the heat transfer coefficient from the gas phase to a cylindrical single particle. For the modeling work in this study, the models described above are used in order to respect the intense particle-particle contact in a fluidized bed. CoolProp [27], an open-source thermophysical property library, was used to calculate properties of the N_2 used as fluidization agent. This allows calcu-

Table 2
Experimental conditions (U: Fluidization velocity, U_{mf}: Minimal fluidization velocity, d: Mean particle diameter, L: Mean particle length, m: Mean particle mass, X_{char}: Char yield).

	Case		1	2	3	4	5	6	7
	Temperature	[K]	673	773	773	773	773	873	773
FLUID	U/U_{mf}	[-]	3.00	1.50	2.25	3.00	3.75	3.00	3.00
	U	[cm/s]	11.43	5.63	8.44	11.25	14.06	11.16	11.25
	U_{mf}	[cm/s]	3.81	3.75	3.75	3.75	3.75	3.72	3.75
BIOMASS	d	[mm]	6	6	6	6	6	6	6
	L	[mm]	21.8	22.2	22.1	22.1	22.2	22.2	8.3
	m	[g]	0.75	0.76	0.76	0.76	0.76	0.76	0.28
CHAR	d	[mm]	5	–	4.8	4.7	4.8	5.1	–
	L	[mm]	21.0	–	19.7	20.3	20.3	20.9	–
	m	[g]	0.24	–	0.21	0.19	0.18	0.15	–
	X_{char}	[%]	32.58	–	27.16	25.41	23.38	20.00	25.41

Table 3
Adapted model properties [15] and biomass composition for softwood and hardwood [25].

Model properties			
Density solid biomass	[kg/m^3]	1500	
Density solid char	[kg/m^3]	1500	
Initial porosity	[-]	Adapted to reach desired pellet density	
Minimum shrinkage factor	[-]	0.46	
Heat capacity biomass	[J/(kg*K)]	1500 + T	
Heat capacity char	[J/(kg*K)]	420 + 2.09 * T – 6.85 * 10^{-4} * T^2	
Heat capacity moisture	[J/(kg*K)]	4200	
Thermal conductivity biomass	[W/(m*K)]	0.177 (softwood pellets)	
Thermal conductivity char	[W/(m*K)]	0.1	
Permeability biomass	[m^2]	1 * 10^{-12}	
Permeability char	[m^2]	1 * 10^{-10}	
Pore diameter	[m]	1 * 10^{-4}	
Emissivity	[-]	0.9	
Dynamic viscosity gas	[kg/(m*s)]	1 * 10^{-5}	
Thermal conductivity gas	[W/(m*K)]	0.0258	
Initial temperature	[K]	300	
Biomass composition		Hardwood	Softwood
Cellulose	[m% ash-free]	44.0	44.0
Hemicellulose	[m% ash-free]	34.0	26.0
LIG-C	[m% ash-free]	6.0	17.5
LIG-H	[m% ash-free]	7.0	9.5
LIG-O	[m% ash-free]	9.0	3.0

lating temperature dependent values of density, dynamic viscosity and thermal conductivity required by the heat transfer models.

For a reasonable characterization of the temperature profile in the particle, accurate physical properties are crucial. Many studies found in literature investigate the thermal conductivity in raw wood which differs strongly from wood pellets. The anisotropic nature of raw wood leads to a thermal conductivity in direction of the fibers which can be 2.5–3 times higher than in the perpendicular direction [28]. The thermal conductivity of single biomass particles is studied in [28] via a measurement method that includes the milling and homogenization of the material. For a softwood pellet with a density of 1179 kg/m^3 the thermal conductivity was measured to be $\lambda_{biomass} = 0.177$ W/(m * K) [28]. As the particle density of 1213 kg/m^3 for the pellets used in this study is very similar, this value will be used for all of the modeling work conducted with softwood pellets. Since different fuels were employed in some of the experimental work from literature modeled in this study, appropriate values for thermal conductivity need to be used. For simulations using beech particles, the thermal conductivity of beech $\lambda_{biomass} = 0.14$ W/(m * K) given by Di Blasi and Branca [12] was employed. The thermal conductivity for cardoon pellets was not found in literature, thus, a representative value of $\lambda_{biomass} = 0.26$ W/(m * K) was employed for simulations with cardoon pellets. The thermal conductivity of char was chosen to be $\lambda_{char} = 0.1$ W/(m * K) which is similar to the value employed by Anca-Couce et al. [15]. The model uses an averaged thermal conductivity, which is calculated for each control volume by weighting the thermal conductivities of biomass and char during conversion.

4. Results and discussion

4.1. Experimental results from this work

The influence of bed temperature, fluidization velocity and pellet size on the mass loss (dashed line) and the conversion (solid line) of the biomass in the fluidized bed experiments introduced in Section 3.1 is presented in Fig. 4. As the mass signal measured by the balance is fluctuating due to the bubbles in the bed, the curves show averaged values to facilitate the evaluation. The mean deviation of the measured mass loss signal is shown as the shaded area.

Fig. 4a shows a strong influence of reactor temperature on the pyrolysis of biomass. The final mass of char measured at the end of each experiment is used to calculate the pyrolysis degree of conversion in order to facilitate the comparison of the different cases. The evolution of the degree of conversion is as well depicted in Fig. 4 for each case. As expected, higher temperatures lead to faster conversion and lower char yields. The influence of the fluidization velocity is depicted in Fig. 4b. The effect of the gas velocity on the pyrolysis conversion is small for velocities bigger than $U/U_{mf} = 1.5$ but much more distinct when U gets closer to U_{mf}. It was already seen in Fig. 1 that the heat transfer coefficient increases signifi-

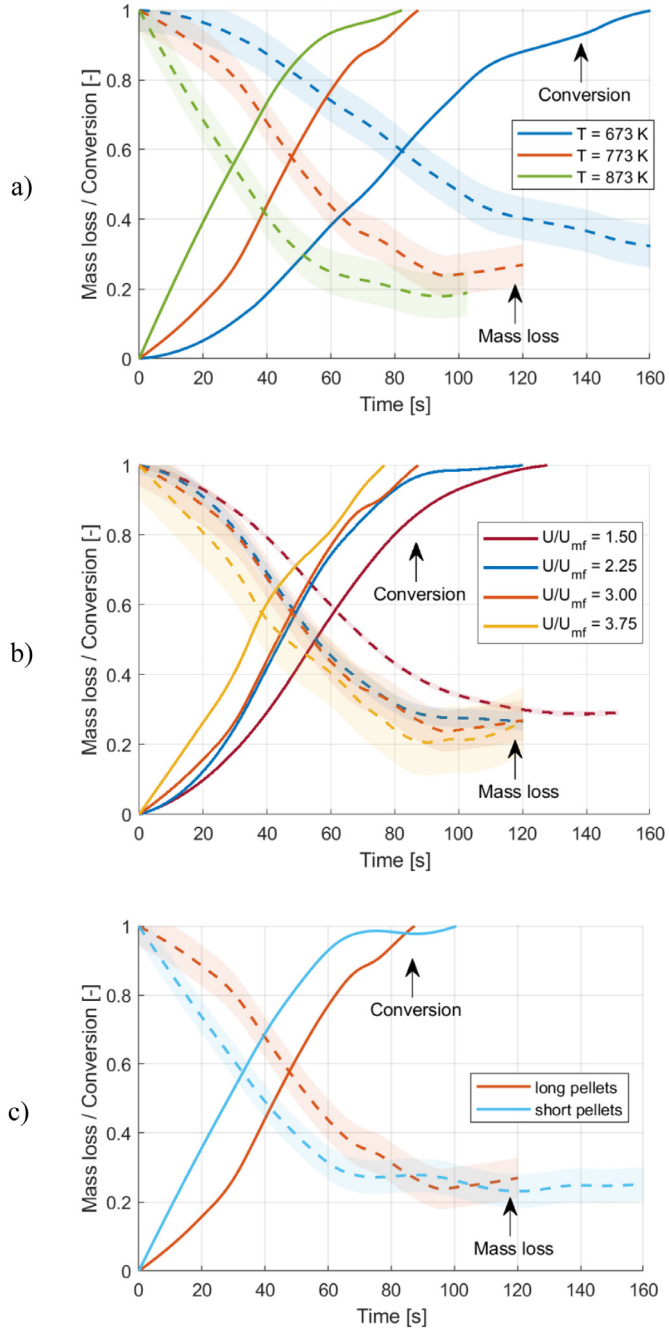

Fig. 4. Comparison of the mass loss (dashed line) and conversion (solid line) for a) $U/U_{mf} = 3$ and various temperatures, b) $T = 773$ K and various gas velocities and c) effect of the pellets size on the pyrolysis process (shaded areas show standard deviation of the measurements).

cantly at velocities just above U_{mf}. For higher ratios of U/U_{mf} this effect is not that distinct anymore which leads to a lower influence on the overall pyrolysis process. The vibrations observed in the measured mass signal are stronger for high gas velocities due to the presence of larger bubbles in the bed. This leads to a higher mean deviation for higher fluidization velocities.

In addition to the tests conducted using pellets of about 22 mm length, another test was conducted at 773 K and $U/U_{mf} = 3$ but with a pellet length of 8.3 mm. The effect of the pellets size on the pyrolysis process can be observed in Fig. 4c. The pyrolysis process is faster for the short pellets due to the larger surface to volume ratio of these pellets, which leads to higher heating rates compared to the long pellets.

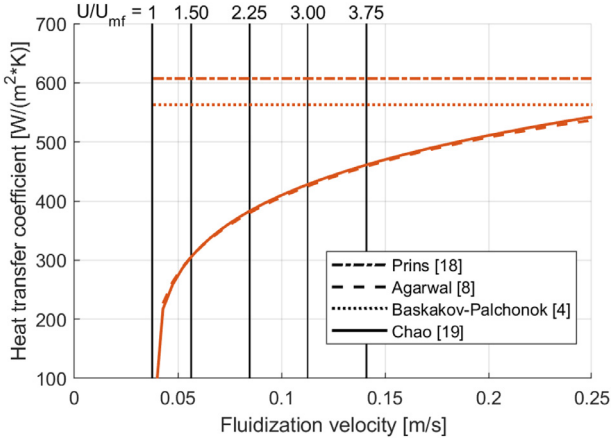

Fig. 5. Comparison of heat transfer correlations using experimental conditions of this study at 723 K.

4.2. Modeling results

In the following section, modeling results are compared with measurement data conducted in this study and from literature. The importance of a model which represents temperature gradients in the particle is highlighted. Furthermore, the influence of the heat transfer model regarding cases with U/U_{mf} ratios slightly higher than one are investigated in more detail. Additionally, the case of conditions at the minimum fluidization velocity as well as for a fixed bed is evaluated. An overview of the different experimental data sources used to validate the modeling results is given in Table 4. In addition to the measurements conducted during this study, the model was also validated using experimental data presented by Di Blasi and Branca [12], Reschmeier et al. [13] and Morato-Godino et al. [14]. Overall, this results in a thorough assessment of the model in regards of reactor temperature, biomass feedstock, particle dimensions and fluidization velocity.

4.2.1. Comparison with softwood experiments from this work

The experimental set-up and the operating procedure of this study were presented in chapter 3.1 and the measurement results were already discussed in chapter 4.1. The input data necessary for the single particle model can be found in Table 3. As softwood pellets were used, the biomass composition presented for softwood was used for the calculations. Other case-dependent input parameters like reactor temperature, fluidization velocity and initial pellet size can be found in Table 2. To better understand the effect of the heat transfer correlation for the experimental conditions used in this study, the different models are compared in Fig. 5 for the employed sizes of bed material and biomass particles. The Sauter diameter was used as a representative diameter of the cylindrical biomass pellets and an average bed material diameter of $d_i = 275$ μm was employed. The shown values are valid for a temperature of 773 K. However, the tendencies are the same for temperatures of 673 and 873 K. Higher temperatures lead to slightly higher heat transfer coefficients and lower temperatures result in slightly lower values. Furthermore, the minimum fluidization velocity U_{mf} and the ratios of U/U_{mf} used during the experiments are marked via vertical lines and labeled at the top of the diagram. The models of Prins and Baskakov-Palchonok are not dependent on fluidization velocity and lead to a rather high heat transfer coefficient. The models of Chao and Agarwal give very similar results. Both show a fast increase of the heat transfer coefficient just above U_{mf}, which then approaches the values of the two other models at high fluidization velocities. Therefore, the main difference between the models will occur at low fluidization velocities whereas for high

Table 4
Experimental conditions of measurements conducted in this study, by Di Blasi and Branca [12], Reschmeier et al. [13] and Morato-Godino et al. [14].

		This study	Di Blasi [12]	Reschmeier [13]	Morato-Godino [14]
Method					
		Gravimetric	Temperature at particle centre	Gravimetric	Gravimetric
Biomass					
Material	[-]	Spruce pellets	Beech wood (no pellets)	80% spruce 20% pine	Cardoon pellets
Shape	[-]	cylindrical	cylindrical	cylindrical	cylindrical
Diameter	[mm]	6	2 to 10	6	6
Length	[mm]	22; 8	20	20	18
Total mass	[g]	~ 7.5 g (10 pellets)	1 Particle	~ 50 g	~10 g
Position in Reactor	[-]	Free	Fixed at 3.5 cm above distributor	Free	Free
Moisture	[%]	8	0 (dried at 373 K)	8	0 (dried at 377 K)
Reactor					
Diameter	[mm]	47	63	50	47
Height	[mm]	500	450	120	500
Bed					
Temperature	[K]	673 to 873	712 to 1107	523 to 923	723 to 923
Bed material	[-]	Sand	Sand	Quartz sand	Sand
Total mass	[g]	257	–	–	250
Height of fixed bed	[mm]	94	–	–	100
Diameter	[my]	275 +/−100	180–250	60–200	390
Particle density	[kg/m^3]	2600	–	–	2600
Bulk density	[kg/m^3]	1576.3	1650	–	–
U_{mf}	[cm/s]	3.72 to 3.81	3.6	3.25	3.41 to 4.00
Gasflow					
U/U_{mf}	[-]	1.5; 2.25; 3.0; 3.75	8	4.9	~0.5 to ~3.7
Fluid	[-]	N_2	N_2	N_2	N_2

ratios of U/U_{mf} the influence will be smaller. As a reference, the heat transfer model by Agarwal was used for all simulations. For two selected cases, the results derived from all four of the different heat transfer models are compared to each other.

To evaluate the importance of different heat transfer mechanisms, the Biot number of the reference case conducted at 773 K employing a gas velocity of $U/U_{mf} = 2.25$ was investigated. The Biot number can be understood as the ratio of the thermal resistivity inside the solid material by conduction R_{th} to the resistance to heat transfer by convection at its surface R_s [29]. For very low Biot numbers, particles are called thermally thin and internal temperature gradients are not present, obtaining a rather uniform temperature inside the particle controlled by external convection. For high Biot numbers, particles are called thermally thick, heat transfer by conduction inside the solid particle is more important and thermal gradients will be present.

$$Bi = \frac{R_{th}}{R_s} = \frac{\frac{L_c}{\lambda_{biomass}}}{\frac{1}{h}} = \frac{h * L_c}{\lambda_{biomass}} \tag{9}$$

Here, L_c represents the characteristic length of the particle, which, in case of a cylinder, can be chosen to equal the cylinder radius [12]. Assuming a thermal conductivity of $\lambda_{biomass} = 0.177$ W/(m * K) and using the Agarwal model to calculate the heat transfer coefficient $h = 383$ W/(m^2*K), the resulting Biot number for a cylinder with 3 mm radius equals $Bi \approx 6$. This is well above the limit of thermally thin particles of about 0.1, for which inner-particle temperature gradients could be neglected [30]. For thermally thin particles, assumptions to simplify the solution of the heat transfer problem are applicable and therefore the mathematical modeling complexity can be decreased. Otherwise, the solution could be simplified in the case of high Biot numbers as in this case internal heat transfer by conduction is much more important. However, as shown above, in the case of biomass pellets inside a fluidized bed, the Biot number close to one indicates the requirement of a more sophisticated heat transfer modeling.

Fig. 6a shows modeling results (solid line) and the corresponding experimental data (dashed line) for different temperatures at a fixed gas velocity of $U/U_{mf} = 3$. In general, the influence of reac-

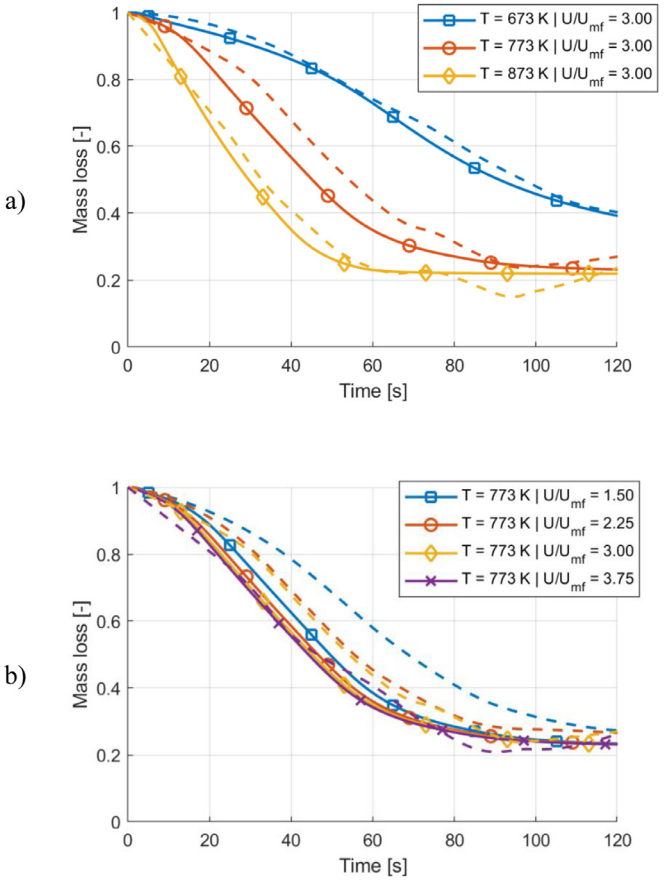

Fig. 6. Comparison of modeling results (solid line) with experiments (dashed line) conducted in this study: a) Temperature variation at $U/U_{mf} = 3$, b) Variation of fluidization velocity at 773 K (HTM: Agarwal, $\lambda_{biomass} = 0.177$ W/(m*K)).

tor temperature can be accurately described by the model. At the beginning of each experiment, a slower rate of mass loss due to particle heat-up and evaporation of moisture can be seen. Afterwards, devolatilization of biomass, strongly dependent on reactor temperature, takes place. The mass loss in the end of each experiment determines the amount of char obtained during the pyrolysis process. Good agreement can be seen for all three of these phases. In order to quantify the deviation and to facilitate the comparison of modeling and experimental results, the following measure was defined.

$$\text{Deviation} = 100 * \frac{\sum |\text{Experimental result } (t) - \text{Modeling result } (t)|}{\text{Total number of temporal samples}} \quad (10)$$

The calculation was performed using a value at each second of the test which leads to a total number of temporal samples of 120. For Fig. 6a, the deviation for each case at temperatures of 673, 773 and 873 K is calculated as 2.1, 5.1 and 3.1%, respectively. The influence of the fluidization velocity investigated at 773 K is shown in Fig. 6b. An acceptable agreement can be found for all cases except for very low gas velocities of $U/U_{mf} = 1.5$. The experimental data shows a stronger influence of reducing the gas velocity than the model. This may be attributed to the soft fluidization induced by this low gas velocity, for which small bubbles are present in the bed, in contrast to the vigorous fluidization obtained for higher values of U/U_{mf}. The reduction of bubbles size for $U/U_{mf} = 1.5$ results in a significant reduction of the mixing in the bed, which affects the dispersion of the biomass particles supplied as a fuel. The cases presented in Fig. 6b showing increasing fluidization velocities of $U/U_{mf} = 1.50,\ 2.25,\ 3.00$ and 3.75 lead to a deviation of 10.3, 5.9, 5.1 and 2.7%, respectively.

To further investigate the influence of the heat transfer model, a comparison of the four different correlations is shown in Fig. 7a. The experimental conditions using a reactor temperature of 773 K and a rather fast fluidization of $U/U_{mf} = 3.75$ was used as a reference. As already seen in Fig. 5, the difference between the models is small for high fluidization velocities. The model by Agarwal and Chao predict heat transfer coefficients of 464 and 476 W/(m^2*K), respectively, and lead to almost the same result. Prins and Baskakov-Palchonok models predict heat transfer coefficients of 621 and 570 W/(m^2*K), respectively. Due to the slightly higher heat transfer coefficient, the pyrolysis process estimated using these two later heat transfer models is faster compared to the results using correlations by Agarwal or Chao. However, all models show good agreement with experimental results. For all four correlations, the modeling results lay within the standard deviation of the experimental data. Deviation from experimental data when using the different heat transfer models of Prins, Baskakov-Palchonok, Chao and Agarwal is calculated as 3.6, 3.3, 2.7 and 2.7%, respectively. The model of Agarwal followed by the one Chao shows best agreement with measurement data, however, all models lead to a similar result.

The influence of the different heat transfer models when employing a rather low fluidization velocity of $U/U_{mf} = 1.5$ is shown in Fig. 7b. None of the four models previously used is able to match the measurements. Correlations by Prins and Baskakov-Palchonok lead to the same heat transfer coefficients of 621 and 570 W/(m^2*K), respectivelly, since no fluidization velocity effect is considered in these correlations. Both cases lead to a devolatization significantly faster than the experimental data. Due to their dependency on the fluidization velocity, the models of Agarwal and Chao result in heat transfer coefficients of 318 and 313 W/(m^2*K), respectively. These modeling results are closer to the experimental data than the ones of Prins and Baskakov-Palchonok, however, the deviation is still high. Fig. 5 shows that for low ratios of U/U_{mf},

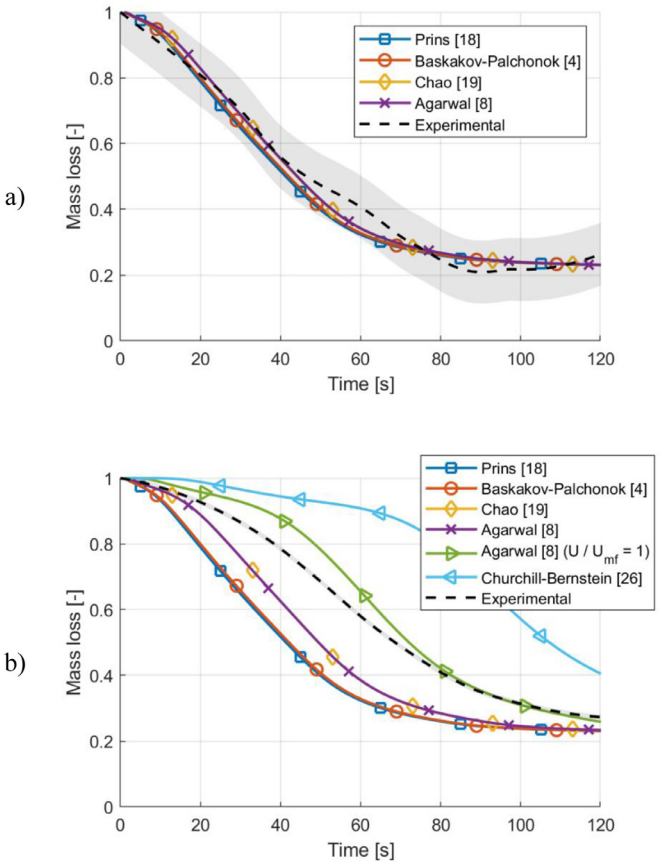

Fig. 7. a) Comparison of heat transfer coefficient at high fluidization velocity ($U/U_{mf} = 3.75$) and reactor temperature of 773 K, b) Comparison of heat transfer coefficient at low fluidization velocity ($U/U_{mf} = 1.5$) and reactor temperature of 773 K (shaded areas show standard deviation of the measurements).

even small differences in velocity lead to significant changes in the heat transfer coefficient. Due to the soft fluidization induced for a gas velocity of $U/U_{mf} = 1.5$, characterized by the presence of small bubbles, the bed might not be mixed homogeneously. This can especially be true for low fluidization velocities and binary mixtures as shown in [31]. For places with locally lower mixing, the heat transfer to the biomass particles will also be reduced. Therefore, the model by Agarwal was employed again for the exactly same input parameters but using a ratio of $U/U_{mf} = 1$ instead. These simulation results show much better agreement with experimental data. Moreover, the speed of pyrolysis is now slightly underestimated. The experimental data lies within the two modeling results using the Agarwal model. This seems reasonable as in the experimental test, the fluidization behavior and particle distribution in the bed can also be described as a mixture of these two cases. For comparison, modeling results when employing the Churchill-Bernstein [26] model are also shown. This model is applicable for the heat transfer to a single cylindrical particle where no interactions with any other particles take place. The correlation leads to a heat transfer of 22 W/(m^2*K), significantly lower than for all of the other models. It is clear that the model is not suited for this application and a strong deviation to the experimental results can be seen. The deviation from experimental data when comparing modeling results using the heat transfer models of Prins, Baskakov-Palchonok, Chao, Agarwal, Agarwal ($U/U_{mf} = 1$) and Churchill-Bernstein is calculated as 15.3, 14.8, 10.3, 10.3, 3.7 and 21.1%, respectively. Except for the case of the Agarwal model

at $U/U_{mf} = 1$, all models show significant deviation from the measurement.

Overall, it was observed that the influence of the different heat transfer models is not significant for high gas velocities and all models lead to acceptable results. For small fluidization velocities, the models by Agarwal and Chao give considerably better results, however, there is still a clear deviation to the experimental results.

4.2.2. Comparison with experimental results of Di Blasi and Branca

The pyrolysis experiments of Di Blasi and Branca [12] were conducted using a single beech wood cylinder in a nitrogen blown fluidized bed. Sand is used as bed material and the fluidization velocity is set for each case in order to achieve a ratio of $U/U_{mf} = 8$. The particle was located in a fine mesh at a fixed position 3.5 cm above the gas distributor. Therefore, it was not allowed to move freely in the bed which might influence the pyrolysis process. The temperature in the center of the particle was measured via a thermocouple inserted through a drilled hole. The results presented by Di Blasi and Branca for a variation of the cylinder diameter ranging from $d = 2$ to 10 mm were used for validation purposes. The length of the cylinder was kept constant for all experiments, which were conducted at a reactor temperature of 807 K. In order to respect the biomass composition of beech wood, the representative biomass composition of hardwood presented in Table 3 is used as a model input. In the case of raw wood, the thermal conductivity in direction of the fiber can be 2.5 to 3 times higher than in radial direction [28]. As the particle model does not consider different thermal conductivities in radial and longitudinal direction, the averaged value stated by Di Blasi and Branca of $\lambda_{biomass} = 0.14$ W/(m*K) was used. The heat transfer coefficient was calculated using the model of Agarwal for all cases.

Fig. 8a shows the experimental and modeling results for different cylinder diameters. A fast temperature increase at the beginning adjourned by a short phase with lower gradient is followed by a second fast increase of temperature. According to Di Blasi and Branca, the lower slope can be explained by the onset of endothermic degradation of holocellulose. The exothermal peak at the end of the experimental data can also be correctly described by the model for most of the cases. The endothermic and exothermic behavior of the pyrolysis model used in the present study was investigated in [32], where it is shown that this temperature increase at the end of conversion can be attributed to exothermic charring reactions. In general, the temperature in the particle center can be well predicted by the model. However, for small particles up to 4 mm diameter, the model projects a significantly faster pyrolysis. A 0.5 mm hole was drilled into each particle to allow measurement of the center temperature. Deviations may be attributed to the higher influence of the temperature probe for small particles. The discrepancy between measurement results and simulation for small particles might also be partly due to the anisotropic nature of raw wood. For high ratios of cylinder diameter versus length, the employed averaged properties, e.g. for thermal conductivity, might not be valid. Anyhow, for the particles in a size range close to the ones in the previous section, an excellent agreement is found.

4.2.3. Comparison with experiments of Reschmeier et al.

Reschmeier et al. [13] used an experimental rig based on the measurement of the mass signal during the pyrolysis process very similar to the one used in this study. Sand was used as bed material and nitrogen as the fluidizing agent. The flow rate was kept at a constant ratio $U/U_{mf} = 4.9$ while the temperature was varied between 623 and 873 K. Softwood pellets of 6 mm diameter were used as feedstock and the biomass composition for softwood proposed in Table 3 is used for modeling. The length of pellets employed was not stated by Reschmeier et al. However, a parameter study showed almost identical modeling results when employing particle lengths of 15, 20 and 25 mm. This was also found by Gómez-Barea et al. in [9], where several tests varying the pellets length while maintaining the batch size showed no significant effects on product yield or conversion time. Therefore, a length of 20 mm, typical for commercial wood pellets, was used. Heat transfer was modeled using the Agarwal correlation and the thermal conductivity $\lambda_{biomass} = 0.177$ W/(m*K) measured by Mason et al. [28] for pelletized softwood was used. Fig. 8b shows the mass loss during the pyrolysis process. An excellent agreement of experimental and modeling data can be seen for all temperatures.

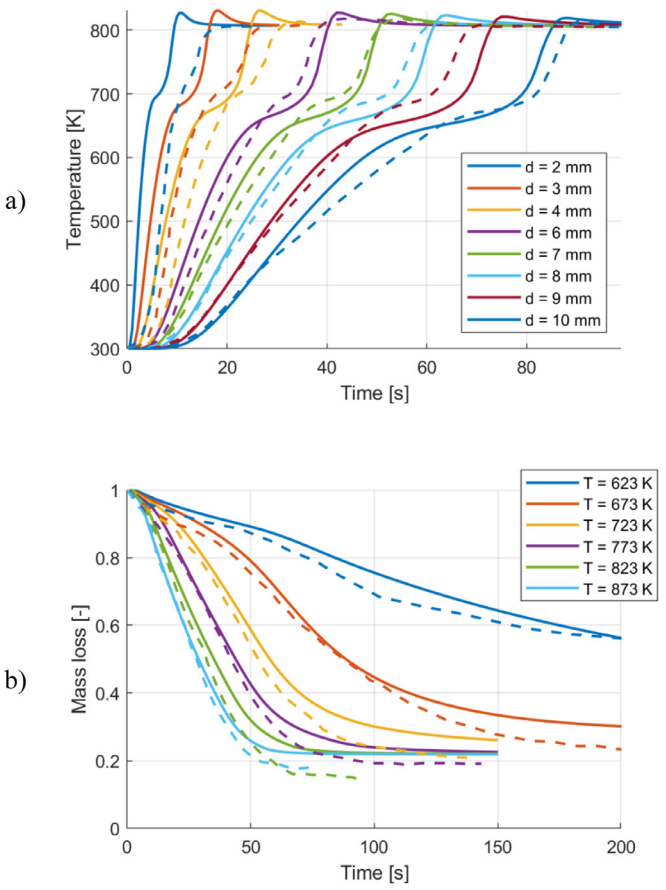

Fig. 8. Comparison of modeling results (solid line) with experiments (dashed line): a) Di Blasi and Branca [12] ($T = 807$ K, HTM: Agarwal, $\lambda_{biomass} = 0.14$W/(m*K)) and b) Reschmeier et al. [13] ($U/U_{mf} = 4.9$, HTM: Agarwal, $\lambda_{biomass} = 0.177$ W/(m*K)).

4.2.4. Comparison with cardoon experiments by Morato-Godino et al.

The measurement setup used by Morato-Godino et al. [14] is the same as the used for the experiments in this study. The setup consisting of a fluidized bed placed on a balance is explained in the experimental section, more details about the exact operating procedure can be found in [14]. Morato-Godino et al. investigated pyrolysis of 6 mm diameter cardoon pellets at different temperatures, particle lengths and fluidization velocities. Cardoon is a perennial plant adapted to climate conditions of low rainfall and hot dry summers with high potential as a non-food agricultural crop [33]. The biomass composition of hardwood presented in Table 3 was used for modeling as a representative composition of cardoon. Cardoon has a much higher ash content, of about 7%, compared to the other investigated fuels in this study. Therefore, a new inert ash species was included in the single particle model. As no value for thermal conductivity of cardoon pellets was found in literature, a value of 0.26 W/(m*K) was assumed. This is equal to the one used by Gomez-Barea et al. [9] for wood pellets. If not

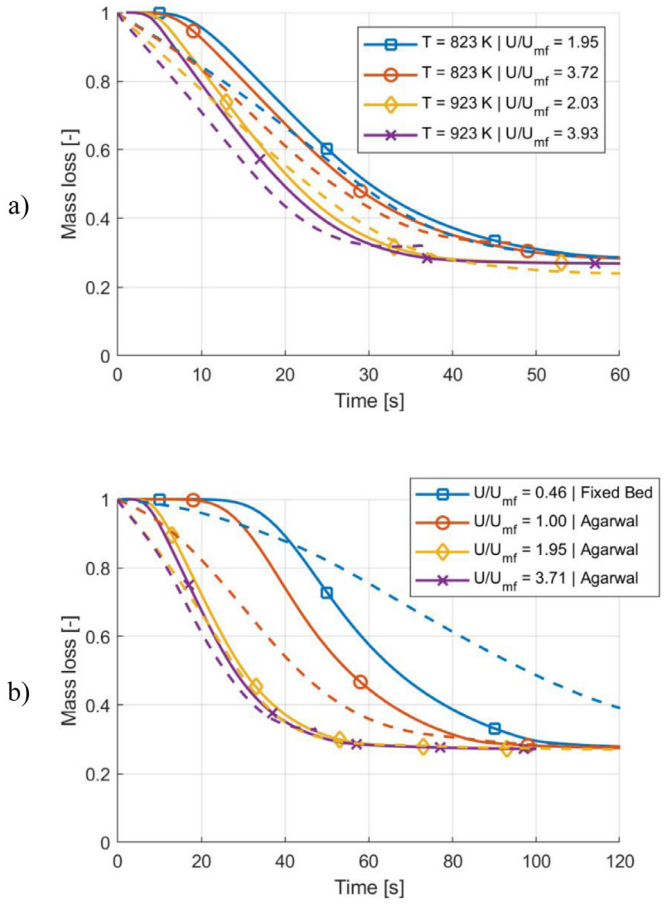

Fig. 9. Comparison of modeling results (solid line) with experiments (dashed line) of Morato-Godino et al. [14]: a) Influence of temperature (HTM: Agarwal, $\lambda_{biomass}$ = 0.26 W/(m*K)) and b) Influence of the fluidization velocity (T = 823 K, $\lambda_{biomass}$ = 0.26 W/(m*K)).

stated differently, the Agarwal model was used for modeling purposes.

To check the validity of the model for cardoon pellets, modeling results are compared to experimental data in Fig. 9a. For reactor temperatures of 823 and 923 K, two different fluidization velocities were employed. Similar to the results shown already, acceptable agreement of experimental and modeling results can be found. The influence of temperature is significant and can be well described by the model. However, the influence of fluidization velocity is slightly underestimated.

To further investigate the influence of the fluidization velocity, two additional tests with lower gas velocity are shown in Fig. 9b for a temperature of 823 K, besides the cases presented at this temperatures in Fig. 9a. For the case of $U/U_{mf} = 0.46$, the bed is not fluidized. As the pellets are fed to the reactor from the top, they are not mixed with the bed material but will stay at the top of the bed and form a fixed bed [14]. Therefore, the heat transfer correlation of Gupta and Thodos [34] suitable for fixed beds was used to model this case. For the case at the minimal fluidization velocity $U/U_{mf} = 1$ the Agarwal model is employed. Distinct deviations are present for both of these cases which emphasizes the difficulty of conditions with low gas velocities. For the test conducted at minimal fluidization velocity, the model predicts slower pyrolysis compared to the experimental data. However, for the test conducted in this study using softwood pellets and a very low gas velocity of $U/U_{mf} = 1.5$ at 773 K, the Agarwal model led to particle conversion faster than in the experiment (see Fig. 7b). Both tests were conducted using 6 mm pellets, but the mean bed material diameter was 275 μm for the tests employing wood pellets and 390 μm for the tests with cardoon. This difference in bed material diameter might lead to a significant influence on the fluidization behavior and may explain partly the differences for those two cases. For the case of a fixed bed, better agreement could be expected. However, for this case the measurement set-up is quite different as the pellets were just accumulated at the top of the bed. This also means that biomass particles in the middle of the pile will not experience same conditions as the ones at the side. This might partly explain the difference to the results of the single particle model.

5. Discussion

As the pyrolysis model was already thoroughly validated, deviations of experimental and modeling data are attributed to the employed heat transfer model. In general, good agreement was found for all different cases when the fluidization velocity was above $U/U_{mf} = 1.5$. Experiments employing different temperatures, biomass diameters typical of pellets, fluidization velocities or fuel-type could be predicted with acceptable accuracy. Furthermore, experimental data obtained using different measurement methods like gravimetric mass loss or temperature measurements were described by the model. Significant discrepancy was found for low gas velocities. However, for most industrial applications, higher gas velocities will be applied. Nevertheless, in some parts of the reactor there might be poorly fluidized areas as shown by Kraft et al. [35] or places with flow regimes close to a fixed or moving bed, e.g. in the loop seal of a dual fluidized bed [36]. Poorly fluidized regions were most probably also present for the tests conducted in this study when employing fluidization velocities below $U/U_{mf} = 1.5$. In such cases, when biomass particles are trapped in dead spots where the bed is not properly fluidized, particle-particle heat transfer will be much smaller and this will significantly influence the conversion process. As the batch size of these experiments was rather small, the effect of a few trapped particles will have significant impact on the measured mass signal. Besides the insecurity regarding the experimental data, the Agarwal model used in this study might also not be applicable for small fluidization velocities. It is a mechanistic model based on bubble parameters like size or velocity which might be problematic at low gas velocities. Another issue might be the density of the biomass particle, which is not considered in the model. As shown by Kunii and Levenspiel [37], the density plays an important role considering the segregation behavior in a fluidized bed. It is shown there that the probability of finding a comparably big particle in a bed of small particles at a certain bed height is significantly influenced by the particle density. Experimental tests showed that particles with a density below 800 kg/m^3 were preferably found at the top of the bed whereas heavier particles are more likely to penetrate deeper into the bed [37]. During the pyrolysis process of a biomass particle, the particle density will change significantly. When using softwood pellets, the initial pellet density of about 1200 kg/m^3 will decrease during pyrolysis to a value around 450 kg/m^3 depending on reactor temperature and fluidization velocity. Therefore, a meaningful improvement might be an adaption of the Agarwal model considering the particle density.

Finally, the time for 50% mass loss of experimental and simulation results for all different experimental campaigns examined in this study is compared in Fig. 10. Regarding the results of Di Blasi and Branca only the modeling work conducted employing a particle diameter of 6 mm is shown, as experimental data for mass loss was not measured. Acceptable agreement can be seen for almost all the results. Even for different biomass types, a clear trend in dependency of temperature can be seen. However, the tests con-

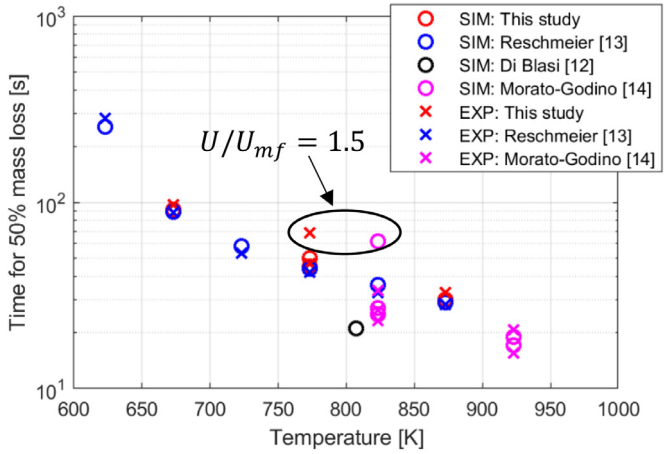

Fig. 10. Time for 50% mass loss of experimental and modeling results (highlighted results employ low fluidization velocity).

ducted at low fluidization velocities below $U/U_{mf} = 1.5$ highlighted in the figure show significant deviations, as previously discussed.

6. Conclusions

Different heat transfer models for fluidized bed conditions found in literature were evaluated and implemented into a single particle model. Therefore, the model by Anca-Couce et al. [15] was adapted to make it applicable for particles in a fluidized bed. Besides, pyrolysis experiments using softwood pellets have been conducted using a fluidized bed installed on a balance at different temperatures and fluidization velocities. The mass loss of several biomass pellets was measured with acceptable repeatability. The single particle model using a heat transfer model developed for conditions in a fluidized bed was able to predict the experimental results of mass loss with a reasonable accuracy. However, significant deviation was found for fluidization velocities close to minimal fluidization ($U/U_{mf} = 1.5$). Additional validation of the model was conducted using experimental data by Di Blasi and Branca [12], Reschmeier et al. [13] and Morato-Godino et al. [14]. Independent of biomass type, a good agreement of experimental and modeling results was found for different reactor temperatures and configurations. Comparison of the temperature at the particle center measured by Di Blasi and Branca also showed acceptable accuracy of the model. The work conducted in this paper showed that in general it is recommended to use an external heat transfer model to the particle considering the fluidization velocity. For high fluidization velocities, the difference between the models was small but in cases where fluidization is poor, the influence of the gas velocity should be considered. However, even though models considering the influence of the gas velocity do lead to a better agreement with experimental data, deviations for these cases are still present.

Future work should implement improvements of the heat transfer models at fluidization velocities close to minimal fluidization. Moreover, the influence of particle shape needs to be investigated in more detail. Furthermore, it is planned to extend the model to make it applicable for fluidized bed gasification. Due to the high temperatures employed for gasification, a detailed description of heat transfer through radiation will be necessary. Finally, the single particle model shall be coupled to CFD models which can describe the detailed hydrodynamics in the bed and the gas phase reactions. This would be an important step towards the detailed modeling of the processes in a fluidized bed at reactor-scale.

Declaration of Competing Interest

The authors declare that they have no known competing financial interests or personal relationships that could have appeared to influence the work reported in this paper.

CRediT authorship contribution statement

Lukas von Berg: Conceptualization, Methodology, Software, Data curation, Writing - original draft. **Antonio Soria-Verdugo:** Investigation, Validation, Writing - review & editing. **Christoph Hochenauer:** Project administration, Supervision. **Robert Scharler:** Funding acquisition, Supervision. **Andrés Anca-Couce:** Methodology, Conceptualization, Supervision, Funding acquisition.

Acknowledgments

This project has received funding from European Union's Horizon 2020 Research and Innovation Programme under grant agreement number 731101 (BRISK II).

References

[1] UNITED NATIONS. Paris Agreement. Paris: 2015.
[2] R Mythili, P Venkatachalam, P Subramanian, D Uma, Characterization of bioresidues for biooil production through pyrolysis, Bioresour Technol 138 (2013) 71–78, doi:10.1016/J.BIORTECH.2013.03.161.
[3] HP Schmidt, A Anca-Couce, N Hagemann, C Werner, D Gerten, W Lucht, et al., Pyrogenic carbon capture and storage, GCB Bioenergy 11 (2019) 573–591, doi:10.1111/gcbb.12553.
[4] A Gómez-Barea, B. Leckner, Modeling of biomass gasification in fluidized bed, Prog Energy Combust Sci 36 (2010) 444–509, doi:10.1016/j.pecs.2009.12.002.
[5] C. Di Blasi, Modeling chemical and physical processes of wood and biomass pyrolysis, Prog Energy Combust Sci (2008), doi:10.1016/j.pecs.2006.12.001.
[6] SRA Kersten, X Wang, W Prins, WPM Van Swaaij, Biomass pyrolysis in a fluidized bed reactor. Part 1: Literature review and model simulations, Ind Eng Chem Res 44 (2005) 8773–8785, doi:10.1021/ie0504856.
[7] C. Di Blasi, Modelling the fast pyrolysis of cellulosic particles in fluid-bed reactors, Chem Eng Sci 55 (2000) 5999–6013, doi:10.1016/S0009-2509(00)00406-1.
[8] PK. Agarwal, Transport phenomena in multi-particle systems—IV. Heat transfer to a large freely moving particle in gas fluidized bed of smaller particles, Chem Eng Sci 46 (1991) 1115–1127, doi:10.1016/0009-2509(91)85104-6.
[9] A Gomez-Barea, S Nilsson, FV Barrero, M Campoy, Devolatilization of wood and wastes in fluidized bed, Fuel Process Technol 91 (2010) 1624–1633, doi:10.1016/j.fuproc.2010.06.011.
[10] FS Mjalli, A. Al-Mfargi, Neural network–based heat and mass transfer coefficients for the hybrid modeling of fluidized reactors, Chem Eng Commun 197 (2010) 318–342, doi:10.1080/00986440903088819.
[11] J Krzywanski, W. Nowak, Modeling of bed-to-wall heat transfer coefficient in a large-scale CFBC by fuzzy logic approach, Int J Heat Mass Transf 94 (2016) 327–334, doi:10.1016/j.ijheatmasstransfer.2015.11.038.
[12] C Di Blasi, C Branca, Temperatures of wood particles in a hot sand bed fluidized by nitrogen, Energy and Fuels 17 (2003) 247–254, doi:10.1021/ef020146e.
[13] R Reschmeier, D Roveda, D Müller, J Karl, Pyrolysis kinetics of wood pellets in fluidized beds, J Anal Appl Pyrolysis 108 (2014) 117–129, doi:10.1016/j.jaap.2014.05.009.
[14] A Morato-Godino, S Sánchez-Delgado, N García-Hernando, A Soria-Verdugo, Pyrolysis of Cynara cardunculus L. samples – Effect of operating conditions and bed stage on the evolution of the conversion, Chem Eng J 351 (2018) 371–381, doi:10.1016/j.cej.2018.06.114.
[15] A Anca-Couce, P Sommersacher, R Scharler, Online experiments and modelling with a detailed reaction scheme of single particle biomass pyrolysis, J Anal Appl Pyrolysis 127 (2017) 411–425, doi:10.1016/j.jaap.2017.07.008.
[16] E Ranzi, A Cuoci, T Faravelli, A Frassoldati, G Migliavacca, S Pierucci, et al., Chemical kinetics of biomass pyrolysis, Energy and Fuels 22 (2008) 4292–4300, doi:10.1021/ef800551t.
[17] M Corbetta, A Frassoldati, H Bennadji, K Smith, MJ Serapiglia, G Gauthier, et al., Pyrolysis of centimeter-scale woody biomass particles: Kinetic modeling and experimental validation, Energy and Fuels 28 (2014) 3884–3898, doi:10.1021/ef500525v.
[18] W. Prins, Fluidized bed combustion of a single carbon particle, 1987.
[19] J Chao, J Lu, H Yang, M Zhang, Q Liu, Experimental study on the heat transfer coefficient between a freely moving sphere and a fluidized bed of small particles, Int J Heat Mass Transf 80 (2015) 115–125, doi:10.1016/j.ijheatmasstransfer.2014.08.049.
[20] J Salinero, A Gómez-Barea, D Fuentes-Cano, B Leckner, The effect of using thermocouples on the char particle combustion in a fluidized bed reactor, Fuel 207 (2017) 615–624, doi:10.1016/j.fuel.2017.06.085.

[21] G.I. Palchonok, A.F. Dolidovich, S. Andersson, B. Leckner, Fluidization VII, in: O.E. Porter, D.J. Nicklin (Eds.), Calculation of true heat and mass transfer coefficients between particles and a fluidized bed, Engineering Foundation, New York, 1992, pp. 913–920.
[22] AP Baskakov, BV Berg, OK Vitt, NF Filippovsky, VA Kirakosyan, JM Goldobin, et al., Heat transfer to objects immersed in fluidized beds, Powder Technol 8 (1973) 273–282, doi:10.1016/0032-5910(73)80092-0.
[23] LM Garcia-Gutierrez, F Hernández-Jiménez, E Cano-Pleite, A Soria-Verdugo, Experimental evaluation of the convection heat transfer coefficient of large particles moving freely in a fluidized bed reactor, Int J Heat Mass Transf 153 (2020) 119612, doi:10.1016/j.ijheatmasstransfer.2020.119612.
[24] A Anca-Couce, R Mehrabian, R Scharler, I Obernberger, Kinetic scheme of biomass pyrolysis considering secondary charring reactions, Energy Convers Manag 87 (2014) 687–696, doi:10.1016/J.ENCONMAN.2014.07.061.
[25] A Anca-Couce, I. Obernberger, Application of a detailed biomass pyrolysis kinetic scheme to hardwood and softwood torrefaction, Fuel 167 (2016) 158–167, doi:10.1016/j.fuel.2015.11.062.
[26] SW Churchill, M. Bernstein, A Correlating Equation for Forced Convection From Gases and Liquids to a Circular Cylinder in Crossflow, J Heat Transf 99 (1977) 300–306.
[27] IH Bell, J Wronski, S Quoilin, V Lemort, Pure and pseudo-pure fluid thermophysical property evaluation and the open-source thermophysical property library coolprop, Ind Eng Chem Res 53 (2014) 2498–2508, doi:10.1021/ie4033999.
[28] PE Mason, LI Darvell, JM Jones, A Williams, Comparative Study of the Thermal Conductivity of Solid Biomass Fuels, Energy and Fuels 30 (2016) 2158–2163, doi:10.1021/acs.energyfuels.5b02261.
[29] HD Baehr, K. Stephan, Wärme und Stoffübertragung, 4. Auflage, Berlin New York, 2004.
[30] MG Nugraha, H Saptoadi, M Hidayat, B Andersson, R Andersson, Particle modelling in biomass combustion using orthogonal collocation, Appl Energy 255 (2019) 113868, doi:10.1016/J.APENERGY.2019.113868.
[31] S Puttinger, S Schneiderbauer, L von Berg, S Pirker, Unstable segregation in fluidized beds, in: CFB-11 Proc. 11th Int. Conf. Fluid. Bed Technol., 2014.
[32] A Anca-Couce, R. Scharler, Modelling heat of reaction in biomass pyrolysis with detailed reaction schemes, Fuel 206 (2017) 572–579, doi:10.1016/J.FUEL.2017.06.011.
[33] J Gominho, MD Curt, A Lourenço, J Fernández, H Pereira, Cynara cardunculus L. as a biomass and multi-purpose crop: A review of 30 years of research, Biomass and Bioenergy 109 (2018) 257–275, doi:10.1016/j.biombioe.2018.01.001.
[34] AS Gupta, G. Thodos, Direct Analogy Between Mass And Heat Transder to Beds of Spheres, AIChE J 9 (1963) 751–754.
[35] S Kraft, M Kuba, H Hofbauer, The behavior of biomass and char particles in a dual fluidized bed gasification system, Powder Technol 338 (2018) 887–897, doi:10.1016/j.powtec.2018.07.059.
[36] P Bareschino, R Solimene, R Chirone, P Salatino, Gas and solid flow patterns in the loop-seal of a circulating fluidized bed, Powder Technol 264 (2014) 197–202, doi:10.1016/j.powtec.2014.05.036.
[37] D Kunii, O. Levenspiel, Fluidization Engineering, 2nd Edition, 1994, doi:10.1016/C2009-0-24190-0.